ELSEVIER

Journal of Molecular Catalysis A: Chemical 165 (2001) 55–66

JOURNAL OF MOLECULAR CATALYSIS A: CHEMICAL

www.elsevier.com/locate/molcata

Kinetic investigation of ethylene polymerization catalyzed by nickel-diimine catalysts

Leonardo C. Simon [a], Christopher P. Williams [a], João B.P. Soares [a,*], Roberto F. de Souza [b]

[a] *Department of Chemical Engineering, Institute for Polymer Research, University of Waterloo, 200 University Av. W., Waterloo, Ont., Canada N2L 3G1*

[b] *Instituto de Química, Universidade Federal do Rio Grande do Sul, Av. Bento Gonçalves 9500, Porto Alegre 91501-970, RS, Brazil*

Received 9 June 2000; accepted 11 September 2000

Abstract

The effect of ethylene pressure on the activity of ethylene polymerization with the complex (1,4-bis(2,6-diisopropylphenyl))-acenaphtenediimine-dichloronickel(II) (**1**) and trimethylaluminum was evaluated. At low ethylene concentrations, the polymerization rate is first order with respect to monomer concentration. At higher ethylene concentrations, the polymerization rate has a negative order with respect to monomer concentration. We propose a mechanism where the active sites are in a dynamic equilibrium with latent states, the later having two monomer molecules coordinated to the metal center. In situ spectroscopic observations corroborate the proposed mechanism and show that the cocatalyst nature might affect the ion pair formation.

Keywords: Polymerization; Kinetics; Nickel-diimine; Polyethylene

1. Introduction

The production of commodity polymers has gained new insights over the last two decades with advances on single site metallocenes [1,2] and half-sandwich-amide complexes [3]. Precise control of molecular weight and homogeneous short and long chain branch distributions have led to polyolefinic materials with novel properties [4,5]. A new generation of olefin polymerization catalysts, based on late transition metals like Fe, Ni and Pd, has emerged as an alternative to broaden even more the use of polyolefins [6,7].

Nickel-diimine catalysts are highly active for ethylene polymerization [8]. This system has a unique behavior that makes it possible to tailor-make the short chain branch content in ethylene homopolymerization. The branches are formed with no comonomer addition through a mechanism called chain walking [9–12]. Catalyst structure, cocatalyst type and concentration, polymerization time, temperature and monomer concentration are key variables affecting productivity, molecular weight and chain walking [13–17]. Nickel-diimine-dihalide needs to be activated by a cocatalyst such as methylaluminoxane, alkylaluminum or alkylaluminum halides. The molar ratio between the catalyst complex and the cocatalyst is far below the one used in systems with metallocene catalysts. The molecular weight increases with

* Corresponding author. Tel.: +1-519-888-4567; fax: +1-519-746-4979.
E-mail address: jsoares@cape.uwaterloo.ca (J.B.P. Soares).

1381-1169/01/$ – see front matter
PII: S1381-1169(00)00429-5

polymerization time, and the polydispersity index ranges from 1.4 to values higher than 2.0.

Much has been done to understand the effect of catalyst structure, temperature and monomer concentration on the chain walking mechanism. However, very few studies describe olefin polymerization kinetics [18] with nickel-diimine complexes. Experimental [8,15] and theoretical [19–22] works have shown that the bulky structure of the diimine ligand blocks axial positions in the active site favoring ethylene insertion over chain transfer. It was also shown that the structure of the diimine backbone affects branch formation.

Temperature and ethylene concentration have a major effect over the polymer microstructure and catalyst activity. Increasing polymerization temperature enhances branch formation, decreases molecular weight and broadens molecular weight distribution. The productivity passes through a maximum with increasing temperature [16,17]. Increasing monomer concentration decreases the number of branches in the final polymer, and also decreases the catalyst activity. Peruch et al. have shown a negative order with respect of monomer concentration in the polymerization of 1-hexene with (1,4-bis(2-isopropylphenyl))-acenaphtenediimine-dibromidenickel(II) (**2**) complex activated by methylaluminoxane (MAO) in toluene or chlorobenzene [18]. Schleis et al. reported a drop in activity with increasing monomer concentration in ethylene polymerization with (1,4-bis(2,6-diisopropylphenyl))-diimine-dibromidenickel(II) (**3**) complex activated by MAO in toluene [15].

We propose herein a kinetic model to describe the monomer effect in the activity, showing how the model fits our experimental data for ethylene polymerization and data from Peruch et al. for 1-hexene polymerization. An in situ spectroscopic study was carried out to seek complementary information about the actual polymerization mechanism. The model suggests a mechanism where two monomer molecules lead the active site to a latent state.

2. Experimental

2.1. Materials

All operations were performed under inert atmosphere of argon using standard Schlenk tube techniques or inside a drybox. The nickel-diimine complex (1,4-bis(2,6-diisopropylphenyl))-acenaphtenediimine-dichloronickel(II) (**1**) was synthesized according to the literature [23]. Chlorobenzene, from Aldrich, was dried using 3 Å molecular sieves. Toluene was distilled from metallic sodium. Methylaluminoxane (MAO) (30 wt.% in isoparafin) was supplied by Witco, triisobutylaluminum (TiBA) (neat) by Aldrich, and trimethylaluminum (TMA) (2 M in toluene) by Aldrich. CP grade ethylene and ultra high purity nitrogen, supplied by Praxair, were purified by passing through 3 Å molecular sieves and de-oxygenation catalyst beds.

2.2. Polymerization

Ethylene polymerizations were done using a 500 ml Autoclave Engineering reactor. The temperature was controlled within $\pm 0.5^{\circ}$C of the set point, by heating an electrical jacket and circulation of cooling fluid through an internal coil. A four-blade impeller rotating at 800 rpm was used for agitation. Prior to each reaction, the reactor was heated to 140°C, then was purged three times with nitrogen (10 bar), placed under vacuum for 30 min, and purged again with nitrogen three more times. Chlorobenzene (295 ml) and the cocatalyst were transferred using needles, under nitrogen flux. The agitation was turned on; the reactor was stabilized at the set-point temperature and fed with ethylene. The ethylene flux was monitored using a mass flow sensor (Brooks 5860E) until diluent saturation was reached. This procedure produced the solubility curve of ethylene in chlorobenzene for each temperature and pressure condition used in this work. When the set-point temperature and ethylene saturation were attained, 5 ml of solution containing 3×10^{-6} mol of complex **1** was pumped into the reactor. After 10 min of polymerization time, 25 ml of ethanol was pumped inside the reactor to quench the polymerization, and then the reactor was vented. The liquid was poured inside 500 ml of acidified ethanol (2 wt.% HCl), and kept there until complete precipitation. The polymer was filtered, washed twice with ethanol, and dried under vacuum at 50°C.

In situ UV–VIS spectra of the polymerization media were recorded in a UV-160A Shimadzu spectrometer at 25°C. The polymerization samples were prepared in toluene in the appropriate concentrations

and transferred to the cells. The ^{1}H NMR polymerization samples were prepared directly in 5 mm tubes, and the spectra were recorded in a Varian Inova 300 and in a Varian Gemini 200 spectrometer, in benzene-d_6 at room temperature with chemical shifts being referred to tetramethylsilane. The paramagnetic susceptibility of the reaction was measured using the Evans method [24,25].

2.3. Polymer characterization

The molecular weight (MW) was evaluated by gel permeation chromatography (GPC) with the Waters 150CV system equipped with three columns with differential viscometer and refractive index detectors. Analyses were undertaken using 1,2,4-trichlorobenzene as solvent (with 0.5 g l^{-1} of Irganox 10/10 as antioxidant), at 140°C, and the MWs were calculated using a universal calibration curve built with polystyrene standards. Crystallization analysis fractionation (CRYSTAF) [26] was performed using the Polymer ChAR CRYSTAF 200 equipment. Samples dissolution was done at 160°C for 30 min followed by 60 min of equilibration period at 95°C. The rate of cooling during crystallization was 0.1°C min^{-1}, from 95 to 30°C. The polymer microstructure was analyzed by ^{13}C NMR spectroscopy [27]. The spectra were obtained with a Bruker 300AC spectrometer operating at 75 MHz, at 80 or 120°C, with a 70° flip angle, acquisition time of 1.5 s and delay of 4.0 s. Sample solutions of the polymer were prepared in 1,2,4-trichlorobenzene in a 10 mm tube.

3. Results and discussion

The polymerizations were carried out at 30, 40 or 50°C. Changing the pressure from 1 to 18 bar attained different monomer concentrations, leading to different degrees of branching. Above 60°C, the system lost the character of very high activity, i.e., the activity drops below 1000 $kg_{pol}\,mol_{Ni}{}^{-1}h^{-1}$. At 20°C and below, at reasonable ethylene concentrations for industrial use, the polymer is mainly linear. The molecular weights steadily increase with increasing monomer concentration, and the molecular weight distributions are around 2.

3.1. Catalyst activity

The system productivity is measured in grams of polymer produced per number of moles of nickel complex added to the reactor and the polymerization time in hours. Table 1 shows the obtained experimental results. Increasing the temperature increases the activity. However, the catalyst activity initially increases with ethylene concentration and then drops after passing through a maximum point. At first glance, this is a striking result, suggesting that the monomer is poisoning the active sites.

3.2. Polymerization kinetics analysis

We propose herein a model that describes the kinetics of ethylene polymerization with nickel-diimine systems. The active site consists of the nickel center ligated by the diazadiene ligand, the growing polymer chain and a molecule of ethylene coordinated. Addition of ethylene to the metal–carbon bond leads to chain growth, according the Cossee mechanism [28].

The main propagation reaction is

$$C_n^* + \mathrm{E} \xrightarrow{k_\mathrm{p}} C_{n+1}^* \tag{1}$$

where C_n^* is the active catalyst site with a growing polymer chain of length n, E an ethylene molecule, and k_p the propagation rate.

In a side reaction, more than one ethylene molecule can coordinate to the active catalyst, leading to a latent state instead of propagation. The coordination of a second ethylene molecule is reversible according to the following dynamic equilibrium between the active species and the latent state:

$$C_n^* + m\mathrm{E} \underset{k_\mathrm{c}^-}{\overset{k_\mathrm{c}}{\rightleftarrows}} C_n^\mathrm{E} \tag{2}$$

where C_n^E is a latent state species, m the number of E coordinated to the nickel center required to achieve the latent state, k_c the rate of latent state formation, and k_c^- the rate of latent state consumption.

The total number of sites during polymerization is then made up of catalyst engaged in propagation and latent state species,

$$C^* = \sum_{n=1}^{\infty} C_n^* \tag{3}$$

Table 1
Effect of temperature and monomer concentration on ethylene polymerization catalyzed by Ni-diimine/TMA

Run	Temperature (°C)	Pressure (bar)	[Ethylene] (mol l^{-1})	Productivity ($kg_{pol}\ mol_{Ni}^{-1}\ h^{-1}$)
1	30	1.0	0.21	210
2	30	2.0	0.42	1360
3	30	3.4	0.69	2120
4	30	4.8	0.97	2890
5	30	8.2	1.66	3530
6	30	11.6	2.35	2950
7	30	15.0	3.05	2890
8	30	18.4	3.74	2060
9	40	1.0	0.17	230
10	40	2.0	0.35	1460
11	40	3.4	0.58	3000
12	40	4.8	0.81	3970
13	40	11.6	1.97	3680
14	40	15.0	2.55	3210
15	40	18.4	3.13	3120
16	50	1.0	0.16	110
17	50	2.0	0.32	1560
18	50	3.4	0.53	3120
19	50	4.8	0.74	3590
20	50	8.2	1.27	4420
21	50	11.6	1.80	6020
22	50	18.4	2.87	6710

$$C^{\mathrm{E}} = \sum_{n=1}^{\infty} C_n^{\mathrm{E}} \tag{4}$$

$$C_t^* = C^* + C^{\mathrm{E}} \tag{5}$$

where C_t^* is the total number of catalyst sites added to the system, C^* the total number of catalyst sites engaged in propagation, and C^{E} the total number of latent species.

From Eq. (1), the rate of propagation is

$$R_{\mathrm{p}} = k_{\mathrm{p}} C^*[\mathrm{E}] = k_{\mathrm{p}}[\mathrm{E}](C_t^* - C^{\mathrm{E}}) \tag{6}$$

It is assumed (using the steady state hypothesis) that the concentration of latent state species changes very little after a short initial period. It is also assumed that the rate of latent state species consumption is almost equal to the rate of its formation, and that both rates are much larger then the difference between them. Therefore, the concentration of the latent state species can be calculated as

$$\frac{\mathrm{d}C^{\mathrm{E}}}{\mathrm{d}t} = k_{\mathrm{c}} C^*[\mathrm{E}]^m - k_{\mathrm{c}}^- C^{\mathrm{E}} \approx 0 \tag{7}$$

$$k_{\mathrm{c}}(C_t^* - C^{\mathrm{E}})[\mathrm{E}]^m - k_{\mathrm{c}}^- C^{\mathrm{E}} = 0 \tag{8}$$

$$C^{\mathrm{E}} = \frac{k_{\mathrm{c}} C_t^*[\mathrm{E}]^m}{k_{\mathrm{c}}[\mathrm{E}]^m + k_{\mathrm{c}}^-} \tag{9}$$

Substituting Eq. (9) in Eq. (6) and simplifying, we get

$$R_{\mathrm{p}} = k_{\mathrm{p}}[\mathrm{E}] C_t^* \frac{k_{\mathrm{c}}^-}{k_{\mathrm{c}}[\mathrm{E}]^m + k_{\mathrm{c}}^-} \tag{10}$$

Eq. (10) points out two limiting cases. First, when the ethylene concentration is low, the first term in the denominator of Eq. (10) is much smaller then the second term in the denominator, so the equation simplifies to

$$R_{\mathrm{p}} = k_{\mathrm{p}}[\mathrm{E}] C_t^* \tag{11}$$

Thus, for low ethylene concentration the polymerization rate increases with increasing ethylene concentration.

For high ethylene concentrations, the first term in the denominator is dominant and the rate of polymerization becomes

$$R_{\mathrm{p}} = \frac{k_{\mathrm{p}} k_{\mathrm{c}}^-}{k_{\mathrm{c}}} C_t^*[\mathrm{E}]^{1-m} \tag{12}$$

For $m > 1$, the rate of polymerization decreases with increasing ethylene concentration at high ethylene concentrations.

The two limiting cases described above are evident from the experimental data, shown in Table 1.

The turnover frequency (TOF), obtained from the productivity, is the average rate of polymerization R_p divided per number of moles of catalyst injected. In these systems, only a fraction of the catalyst injected turns into active species; therefore, the kinetic constant determined here implicity includes the catalysts efficiency. Also, these systems exhibit a long life activity, so the relatively short polymerization time of 10 min excludes considerable effects of catalyst deactivation [16,17]. Therefore, the productivity data shown in Table 1 will be described with the following model:

$$\text{TOF} = \frac{\text{Productivity}}{M_{\text{ethylene}}} = \frac{m_{\text{pol}}}{M_{\text{ethylene}} t C_t^*} = \frac{R_p}{C_t^*} = \frac{k_p[\text{E}]}{K[\text{E}]^m + 1} \quad (13)$$

where,

$$K = \frac{k_c}{k_c^-} \quad (14)$$

and m_{pol} is the mass of polymer produced, M_{ethylene} the molecular weight of ethylene, and t the time.

Table 2 shows the values for k_p, K, and m to fit the experimental data. The fitting was done by minimizing the sum of the squares of the differences between the experimental and predicted data. Two sets are presented, the first making m equal to 2, i.e., assuming that two monomer molecules are required in the latent state, and the second allowing m to vary to fit the experimental results. Table 2 summarizes the parameters, and Fig. 1 displays the experimental data in comparison with data predicted by the model using the parameters. As expected, k_p increases with

Table 2
Kinetic parameters obtained from fitting experimental results

Temperature (°C)	k_p[a] (mol s^{-1})	K	m
30	33.40	0.32	2
40	56.86	0.51	2
50	49.08	0.17	2
			Best m
30	33.43	0.32	2.00
40	53.25	0.35	2.32
50	74.08	0.80	1.04

[a] When $m = 2$.

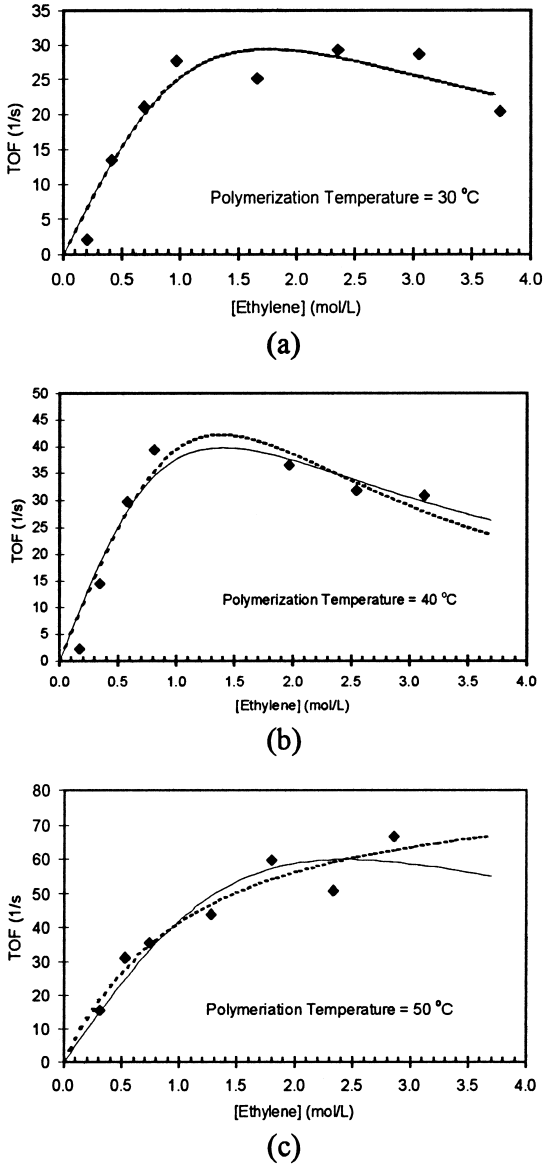

Fig. 1. Effect of monomer concentration on the activity of ethylene polymerization: (a) 30°C; (b) 40°C; (c) 50°C ((◆) experimental; (—) kinetic model with $m = 2$, and (- - -) kinetic model with best m).

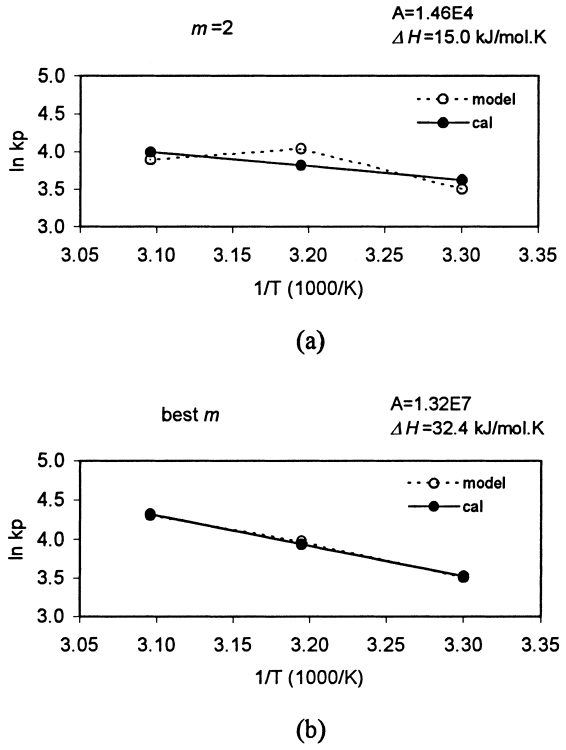

Fig. 2. Arrhenius plot with values predicted by the model (- - - - -) and calculated from equation fitting (—) for: (a) $m = 2$, and (b) best m.

increasing temperature. The activation energy (ΔE_a) and the Arrhenius plot are shown in Fig. 2.

The value of m other than 2, obtained during the best fitting, is more significant at the temperature of 50°C. This can be due to more complex phenomena than the one taken into account in the model, or improper data range.

This kinetic model also fits the literature data presented by Peruch et al. [18] in the polymerization of 1-hexene with another nickel-diimine catalyst activated by MAO in toluene or chlorobenzene. Fig. 3 shows the comparison between experimental results and the predictions of our kinetic model with $m = 2$, i.e., assuming that two monomer units are required to form the latent state.

The formation of latent sites, i.e., reversible deactivation of active sites, has also been proposed in the kinetic investigation of ethylene catalyzed by zirconocene complexes and MAO [29].

3.3. Spectroscopic investigation

According to Brookhart and co-workers, the active catalyst is assumed to be a cationic diimine-nickel species arranged in a square planar geometry with the incoming olefin *cis*-positioned to the metal-bonded growing polymer chain [8].

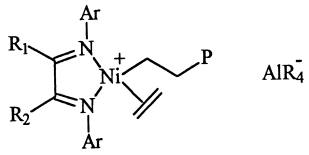

Although, the cation-like mechanism [30] for olefin polymerization catalyzed by early transition metals systems has been largely accepted, the ethene coordinated to the metal center has mainly been observed in nonreactive systems [31,32] or at low temperature [33]. Other intermediates have been observed, such as metal-alkyl-agostic species [34,35], in active polymerization systems. Theoretical studies on the role of ion pairs in the mechanism of olefin coordination polymerization indicated that the noncoordinating counter-anion is involved through olefin-separated ion pairs [36].

We evaluated the ethylene polymerization using in situ UV–VIS and ^{1}H NMR at room temperature, comparing the effect of MAO or TiBA cocatalysts with complex **1**. The NMR spectrometer was also used to measure the paramagnetic susceptibility of the polymerization systems, using the Evans method.

The ^{1}H NMR spectra of the ethene polymerization system obtained with **1**/TiBA show resonances of both free ethene ($\delta = 5.1$ ppm) and coordinated ethene to the nickel complex ($\delta = 4.6$ ppm, [31,32]). The low Al to Ni molar ratio of 0.5, used to slow down the reaction rate in this experiment, probably favors this condition [37] [1] . Under the same reaction conditions, the system **1**/MAO does not show any signal attributed to the coordinated olefin, but a signal due to the free ethene. The reason why only in the system with TiBA, the ethylene coordinated can be observed might be related to the nature of the active species.

[1] The approach of decreasing the cocatalyst to catalyst molar ratio to decrease the activity of the system has also been used for the in situ NMR study of ion pairs in zirconocene-based polymerization systems.

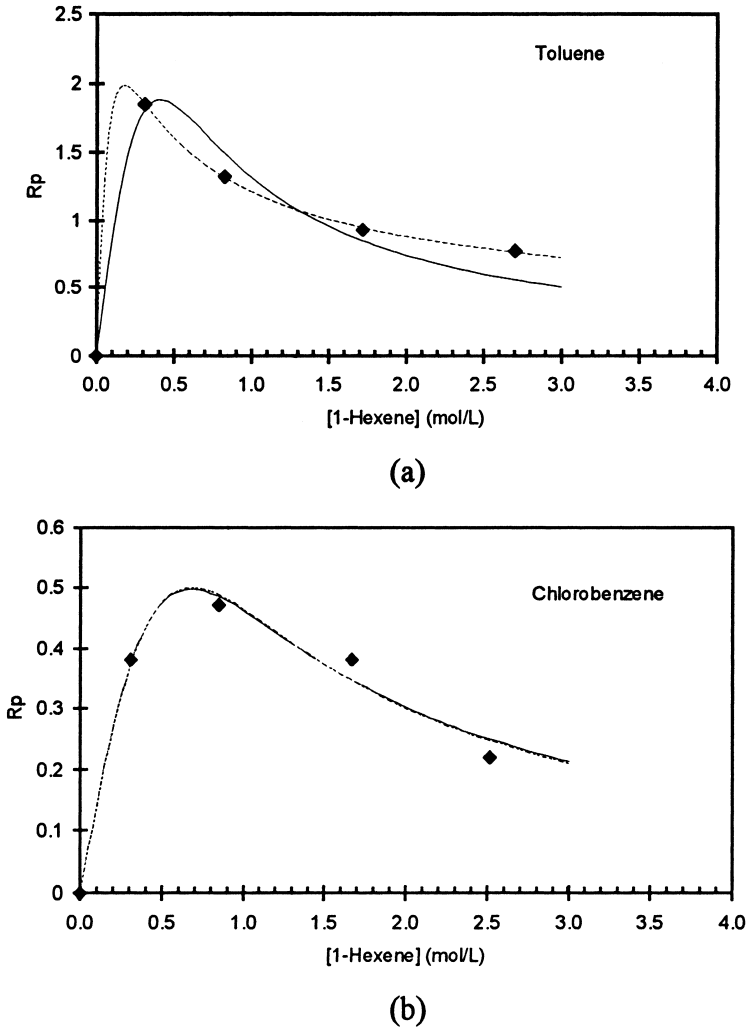

Fig. 3. Effect of monomer concentration on the activity of 1-hexene polymerization in: (a) toluene, and (b) chlorobenzene ((◆) experimental results from Peruch et al. [18]; (—) kinetic model with $m = 2$, and (- - -) kinetic model with best m). The unit of activity is not reported in [18].

Magnetic susceptibility determinations gave values of 2.1 ± 0.1 MB to the complex **1**, in agreement with the tetrahedral symmetry of the analogous complex **3** [15]. The system **1**/ethene/TiBA gives magnetic susceptibility of 1.4 ± 0.1 MB. Therefore, the decrease of the magnetic susceptibility media can be rationalized by an equilibrium between the tetrahedral catalytic precursor **1** (paramagnetic) and the square planar active species (diamagnetic), once both might be present in the system.

The mixture of **1** with MAO or TiBA in the presence of ethene gives different colored systems. The addition of MAO to the orange solution of **1**/ethene turns the solution color to pink, while the addition of TiBA produces a deep blue solution. Fig. 4 shows the UV–VIS spectra of both systems, where the Al to Ni molar ratio is 200. The system with MAO has two bands in the electronic spectra, at $\nu_1 = 18.9 \times 10^3\,\mathrm{cm}^{-1}$ (529 nm) ($\varepsilon_1 = 2797\,\mathrm{l\,mol}^{-1}\,\mathrm{cm}^{-1}$) and $\nu_2 = 14.2 \times 10^3\,\mathrm{cm}^{-1}$ (704 nm) ($\varepsilon_2 = 1838\,\mathrm{l\,mol}^{-1}\,\mathrm{cm}^{-1}$). The system with

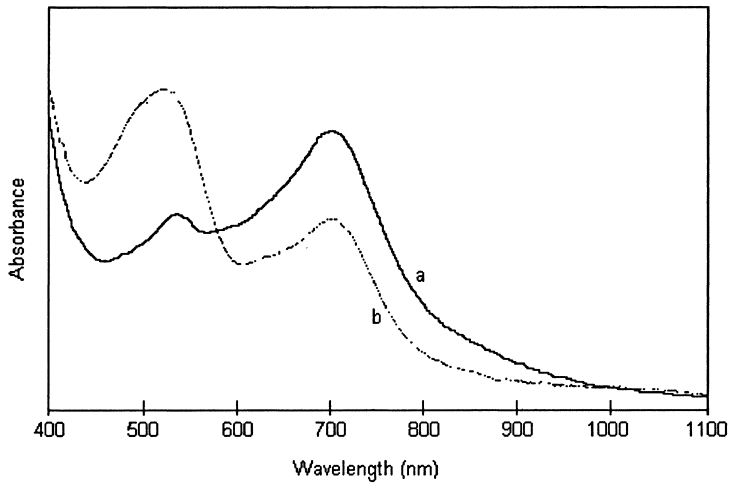

Fig. 4. Electronic spectra of the species formed during ethene polymerization with nickel-diimine complex **1** and TiBA (a) or MAO (b).

TiBA has also two bands, at $\nu_1 = 18.6 \times 10^3\,\mathrm{cm}^{-1}$ (538 nm) ($\varepsilon_1 = 1800\,\mathrm{l\,mol}^{-1}\,\mathrm{cm}^{-1}$) and $\nu_2 = 14.1 \times 10^3\,\mathrm{cm}^{-1}$ (709 nm) ($\varepsilon_2 = 2733\,\mathrm{l\,mol}^{-1}\,\mathrm{cm}^{-1}$). The peak frequencies are nearly the same, but with different intensity with both types of cocatalysts [2]. The difference of intensity of both bands might be an effect of ligands around the nickel core, i.e., due to different degree of ion pair formation between the nickel and the aluminum centers. The nickel-diimine complex **1** does not show any characteristic absorption maximum between 400 and 1100 nm.

Peruch et al. [18] reported the study of polymerization of 1-hexene with the **2**/MAO, and interpreted the electronic spectra as a combination of two species. It was suggested that the active species could be the one exhibiting an absorption at 510 nm, whereas the species corresponding to the band at 710 nm are most likely inactive for polymerization.

The assignment of spectra shown in Fig. 4 to the geometry of the complex is not straightforward. It might not represent an octahedral or a square-planar nickel complex. According to extensive studies done by Sacconi et al. [38], the molar absorption values are too high for a square-planar geometry, and the bands are not characteristic of these geometries as well. Sacconi et al. reported a very similar spectra to the five-coordinated nickel(II) complexes with nitrogen–phosphorous ligands [39]. Drago and Donoghue have shown that $NiLX_2$ complexes (where L = hexamethylphosphoramide and X = Cl, Br, I, NO_3) [40] have a similar electronic spectra, and involve a pseudo-tetrahedral geometry, in between square-planar (C_2v symmetry) and tetrahedral (D_4h symmetry).

The active site is the species involved in a dynamic and continuos process, and its actual picture depends upon the time scale of the experiments used during the investigation.

3.4. Mechanism

We have seen from the kinetic model that the monomer concentration has a direct effect over the mechanism. Spectroscopic observations suggest that the active species are in equilibrium with inactive species. The counter-anion might also affect the nature of the active site.

The mechanism proposed by Cossee for olefin polymerization has a four-center intermediary during the insertion step [28]. Ystenes has proposed the trigger mechanism [41], a modification to the Cossee mechanism. His model is based on the interaction of two

[2] The concentration used to calculate the molar absorptivity (ε) of each system is the concentration of the original complex added to the system. It is expected, however, that only a fraction of the nickel-diimine complex **1** is converted to active species. Hence, the molar absortivity of the active species should be even higher than these reported herein.

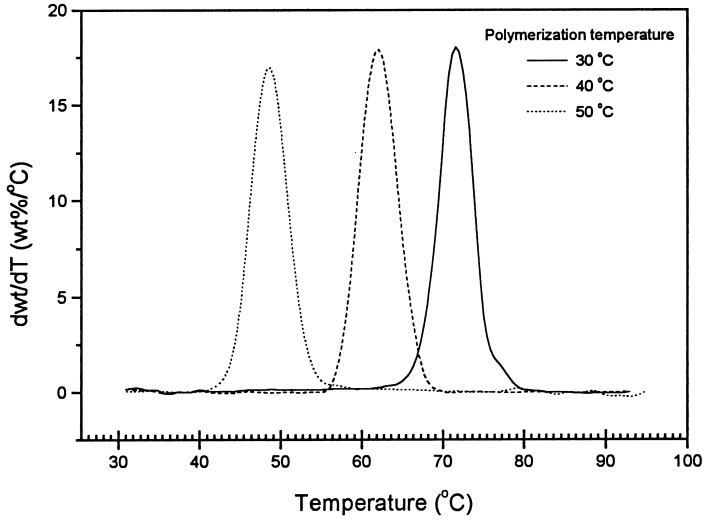

Fig. 5. Chemical composition distribution obtained by crystallization fractionation analysis of polyethylene with different short chain branch content, catalyzed by **1**/TMA at 18.4 bar, and different polymerization temperatures: 30°C (sample 8); 40°C (sample 15), and 50°C (sample 22).

monomer molecules at the transition state, where the monomer activates the active center.

The chemical composition distribution of the polymer presented here, obtained by CRYSTAF, shows only one peak with respect to branch distribution. This is an experimental evidence of only one type of active species. At higher ethylene concentrations, the polymer has low short chain branch content. More branches are formed as the ethylene pressure decreases, shifting the crystallization temperature in solution to lower temperatures. Fig. 5 shows CRYSTAF profiles of some samples from Table 1. The hypothesis of two active sites, one leading to linear polymer and the other to branched polymer, would produce bimodal chemical composition distribution [42], which is clearly not observed with these samples.

Ethylene chain growth promoted by palladium-diimine catalytic systems can be monitored using low-temperature NMR, the active species being characterized in situ. The catalyst resting state is an alkyl olefin complex, and chain growth is dependent only on the rate of migratory insertion [43]. The turnover-limiting step is the migratory insertion reaction of the alkyl ethylene complex, and as a result the chain growth is zero-order in ethylene. Studies of ethylene polymerization, using in situ NMR spectroscopy at −120°C, have shown that the catalyst resting state during chain growth is the alkyl olefin complex [44]. It has been shown by theoretical calculations [20] that during the insertion step, there is a pentacoordinated nickel-diimine center, formed by the growing polymer chain, the coordinated olefin and the agostic hydrogen.

The proposed kinetic model explains the activity dependence on monomer concentration. It shows that in the latent state there might be an interaction of two monomer molecules over the active site, and the stability of this species with two monomer molecules is directly affected by monomer concentration. The latent state is proposed to be a pentacoordinated cationic nickel, with two ethylene molecules coordinated to the metal center. The active sites are the four-coordinated nickel centers, with the diazadiene ligand, the growing polymer chain, and the coordinated ethylene. The coordination of a second ethylene unit leads to the five-coordinated nickel center latent state. The latent state does not allow chain growth. There might be a rapid dynamic equilibrium reaction involving the active and the latent metal centers, as shown in Fig. 6.

In the active site, the coordinated ethylene is inserted in the metal–carbon bond leading to chain growth,

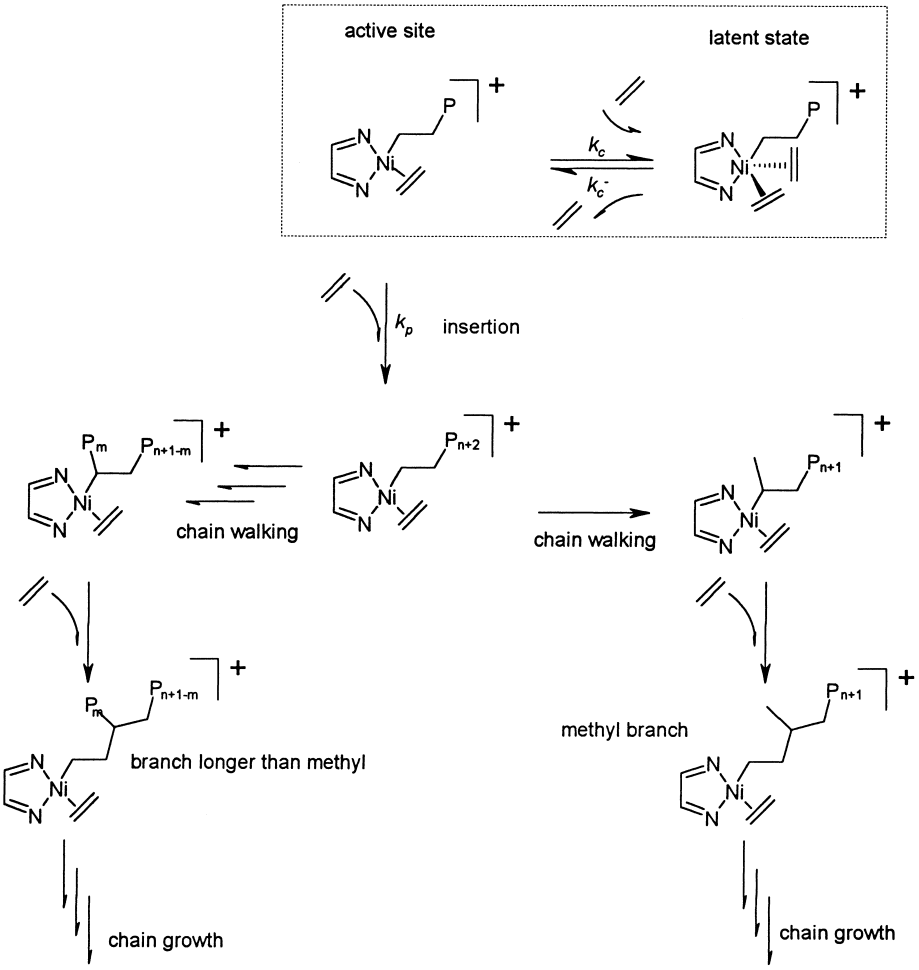

Fig. 6. Proposed mechanism, describing the dynamic equilibrium between active species and latent state for ethylene polymerization with nickel-diimine catalyst.

and the vacant site is supposed to be rapidly trapped by another incoming ethylene. The rate of polymerization is first order with respect to ethylene at low concentrations, therefore, chain growth is favored. At high ethylene concentrations, the latent state competes with the chain growth, decreasing the rate of polymerization. The active sites can also participate in the chain-walking mechanism, producing methyl or longer branches.

The coordination of a second monomer probably blocks the fifth coordination position required during the step of ethylene insertion in the metal–carbon bond (propagation), i.e., the monomer competes with the agostic hydrogen. This might be the reason why the insertion of the ethylene coordinated in the metal–carbon bond is the rate-limiting step.

The nickel-diimine/MAO does not produce polyethylene or copolymer when 5-ethylidene-2-norbornadiene is added [45], if experimental conditions similar to those of ethylene polymerization are used. This mechanism explains why the nickel-diimine/MAO does not have high activity in ethylene polymerization when 5-ethylidene-2-norbornadiene is present. Although, we do not have any spectroscopic observation, we speculate that the bicyclediene would coordinate through both double bonds, slowing down

the insertion step and keeping the metal center permanently at the latent state.

4. Conclusions

The polymerization of ethylene with nickel-diimine catalysts is highly active. The activity has a maximum value with increasing monomer concentration. At low ethylene concentrations, the system follows a first order kinetics with respect to monomer. At higher ethylene concentration, the activity drops when the monomer concentration is raised. We propose a mechanism, where the active sites are in a dynamic equilibrium with a latent state. The latent state might have two ethylene molecules coordinated to the nickel center.

In situ spectroscopic observations are in agreement with other authors' results. The active species might be a cationic alkyl olefin complex, in equilibrium with inactive species. Furthermore, the type of counter-anion might affect the nature of the active species and its equilibrium with the inactive sites.

The narrow chemical composition distribution of the polyethylenes with different degrees of branching indicates that only one type of active site is present in the system.

Acknowledgements

Leonardo C. Simon thanks CAPES Foundation for the fellowship.

References

[1] R. Mülhaupt, in: G. Fink, R. Mülhaupt, H.H. Brintzinger (Eds.), Ziegler Catalysts, Springer, Berlin, 1995, p. 35.
[2] H.H. Brintzinger, D. Fischer, R. Mülhaupt, B. Rieger, R.M. Waymouth, Angew. Chem. Int. Ed. Engl. 34 (1995) 1143.
[3] Y.-X. Chen, T.J. Marks, Organometallics 16 (1997) 3649.
[4] M. Baumert, H. Frey, M. Holderle, J. Kressler, F.G. Sernetz, R. Mülhaupt, Macromol. Symp. 121 (1997) 53.
[5] J.B.P. Soares, A.E. Hamielec, Polym. React. Eng. 3 (1995) 131.
[6] G.P.T. Bristovsek, V.C. Gibson, D.F. Wass, Angew. Chem. Int. Ed. 38 (1999) 428.
[7] S.D. Ittel, L.K. Johnson, M. Brookhart, Chem. Rev. 100 (2000) 1169.
[8] L.K. Johnson, C.M. Killian, M. Brookhart, J. Am. Chem. Soc. 117 (1995) 6414.
[9] M. Brookhart, L.K. Johnson, C.M. Killian, S. Mecking, D.J. Tempel, Polym. Prep. — Am. Chem. Soc., Div. Polym. Chem. 37 (2) (1996) 257.
[10] S.J. McLain, E.F. McCord, L.K. Johnson, S.D. Ittel, L.T.J. Nelson, S.D. Arthur, M.J. Halfhill, M.F. Teasley, D.J. Tempel, C. Killian, M.S. Brookhart, Polym. Prep. — Am. Chem. Soc., Div. Polym. Chem. 38 (1) (1996) 772.
[11] Z. Guan, P.M. Cotts, E.F. McCord, S.J. McLain, Science 283 (1999) 2059.
[12] L.C. Simon, J.B.P. Soares, R.F. de Souza, AIChE J. 45 (2000) 1234–1240.
[13] R.F. de Souza, R.S. Mauler, L.C. Simon, F.F. Nunes, D.V.S. Vescia, A. Cavagnoli, Macromol. Rapid Commun. 18 (1997) 795.
[14] D. Pappalardo, M. Mazzeo, C. Pellecchia, Macromol. Rapid Commun. 18 (1997) 1017.
[15] T. Schleis, T.P. Spaniol, J. Okuda, J. Heinemann, R. Mülhaupt, J. Organomet. Chem. 569 (1998) 159.
[16] L.C. Simon, R.S. Mauler, R.F. de Souza, J. Polym. Sci., Polym. Chem. 35 (1999) 4656.
[17] D.P. Gates, S.A. Svejda, E. Onate, C.M. Killian, L.K. Johnson, P.S. White, M. Brookhart, Macromolecules 33 (2000) 2320.
[18] F. Peruch, H. Cramail, A. Deffieux, Macromolecules 32 (1999) 7977.
[19] L. Deng, T.K. Woo, L. Cavallo, P.M. Margl, T. Ziegler, J. Am. Chem. Soc. 119 (1997) 6177.
[20] D.G. Musaev, R.D.J. Froese, K. Morokuma, New J. Chem. 21 (1997) 1269.
[21] L. Deng, P. Margl, T. Ziegler, J. Am. Chem. Soc. 119 (1997) 1094.
[22] L. Fan, A. Krzywicki, A. Somogyvari, T. Ziegler, Inorg. Chem. 35 (1996) 4003.
[23] G. van Koten, K. Vrieze, in: F.G.A. Stone, R. West (Eds.), Advanced Organometallic Chemistry, Vol. 21, Academic Press, New York, 1982, p. 151.
[24] D.F. Evans, J. Chem. Soc. (1959) 2003.
[25] T.H. Crawford, J. Swanson, J. Chem. Educ. 48 (1971) 383.
[26] B. Monrabal, Macromol. Symp. 110 (1996) 81.
[27] G.B. Galland, R.F. de Souza, R.S. Mauler, F.F. Nunes, Macromolecules 32 (1999) 1620.
[28] P. Cossee, J. Catal. 3 (1964) 80.
[29] K. Thorshaug, J.A. Stovneng, E. Rytter, M. Ystenes, Macromolecules 31 (1998) 7149.
[30] C. Sishta, R.M. Hathorn, T.J. Marks, J. Am. Chem. Soc. 114 (1992) 1112.
[31] Z. Wu, R.F. Jordan, J. Am. Chem. Soc. 117 (1995) 5867.
[32] P.T. Witte, A. Meetsma, B. Hessen, J. Am. Chem. Soc. 119 (1997) 10561.
[33] D.J. Tempel, M. Brookhart, Organometallics 17 (1998) 2290.
[34] G.F. Schmidt, M. Brookhart, J. Am. Chem. Soc. 107 (1985) 1443.
[35] M. Brookhart, A.F. Volpe Jr., D.M. Lincoln, J. Am. Chem. Soc. 112 (1990) 5634.
[36] R. Fusco, L. Longo, F. Mase, F. Garbassi, Macromol. Rapid Commun. 18 (1997) 433.
[37] I. Tritto, R. Donetti, M.C. Sacchi, P. Locatelli, G. Zannoni, Macromolecules 32 (1999) 264.

[38] R. Morassi, I. Bertini, L. Sacconi, Coord. Chem. Rev. 11 (4) (1973) 343.
[39] L. Sacconi, I. Bertini, J. Am. Chem. Soc. 89 (1967) 2235.
[40] J.T. Donoghue, R.S. Drago, Inorg. Chem. 2 (1963) 572.
[41] M. Ystenes, J. Catal. 129 (1991) 383.
[42] J.D. Kim, J.B.P. Soares, J. Polym. Sci., Polym. Chem. 38 (2000) 1427.
[43] D.J. Tempel, M. Brookhart, Organometallics 17 (1998) 2290.
[44] S.A. Svedja, L.K. Johnson, M. Brookhart, J. Am. Chem. Soc. 121 (1999) 10634.
[45] L. D'Agnillo, private communication, 2000.